ICAS 2016
30th Congress of the International Council of the Aeronautical Sciences
DCC, Daejeon, Korea ; September 25-30, 2016

NUMERICAL STUDY OF ACTIVE SHOCK WAVE-TURBULENT BOUNDARY LAYER INTERACTION CONTROL FOR TRANSONIC AERODYNAMICS

Zahra Seifollahi Moghadam *, Alireza Jahangirian **
*** Amirkabir University of Technology, ** Amirkabir University of Technology**

Keywords: *Fluid suction and injection, Transonic flow, Parametric study, Shock wave-*

Abstract

Transonic and high subsonic speeds are from the most critical aircrafts flight conditions due to the fact that flying in these speeds causes local supersonic pockets on their lifting surfaces which end up with a shock wave. Shock wave appearance results in drag increment and has the potential to cause flow unsteadiness and buffet. Shock wave control for large flight vehicles can reduce the fuel consumption and/or alternatively increases the flight range. Therefore, shock waves creation, their interaction with boundary layer and their control have been the subject of the wide range of studies. Surface mass transfer using fluid suction or injection is one of the active devices for the control of shock wave-boundary layer interaction as a means of airfoil drag reduction or aerodynamic performance improvement. A parametric study is carried out in order to gain insight into the effects of mass transfer parameters, i.e. the location, flow rate and the inclination angle on the aerodynamic coefficients. The parametric study is done for off-design transonic flow conditions containing strong shock-boundary layer interaction around the NACA64A010 airfoil and also to determine the required information to commence an optimization process. The flow is simulated by solving the compressible Navier-Stokes equations in Reynolds averaged form together with a two-equation turbulence model. A cell-centered finite-volume scheme is developed with a dual-time implicit time discretization. Results are presented for different mass transfer parameters.

1 Introduction

Shock wave appearance results in drag increment which in one aspect is the result of entropy increment by shock wave presence that leads to wave drag and in another aspect, is the result of shock wave-boundary layer interaction that increases skin friction drag. Thus, on transonic wings, this feature increases the drag.

A wide range of studies are dedicated to study of shock waves ([1], [2], [3]). Several passive and active methods for the control of shock wave and boundary layer interaction and its resultant drag reduction have been presented. Active terms are employed for the methods which can be switched on or off in different conditions.

General methods in the Euroshock project [1] in the area of shock waves drag reduction are illustrated in Fig. 1. These methods include; using a bump to control shock waves, hybrid control of bump and upstream suction, cavity ventilation (transfer of high pressure flow to low pressure region) with downstream suction, passive cavity with inside suction, pneumatic bump and discrete suction upstream of shock wave. Methods such as vortex generators and the passive cavity are examples of passive methods and geometrical and pneumatic bump and flow suction are among active methods. Other ways can be considered as hybrid methods.

One can use pressure difference across the shock to create a flow circulation [3]. This can be obtained by using a cavity and a perforated

plate in the shock wave location. Experimental tests show that pressure increase upstream of the shock (and so Mach number decrease) results in a noticeable decrease in wave drag, although the total drag increases due to an increase in skin friction in the control position. By the placement of suction behind the cavity, the boundary layer is thinned and the obtained results are more favorable [1].

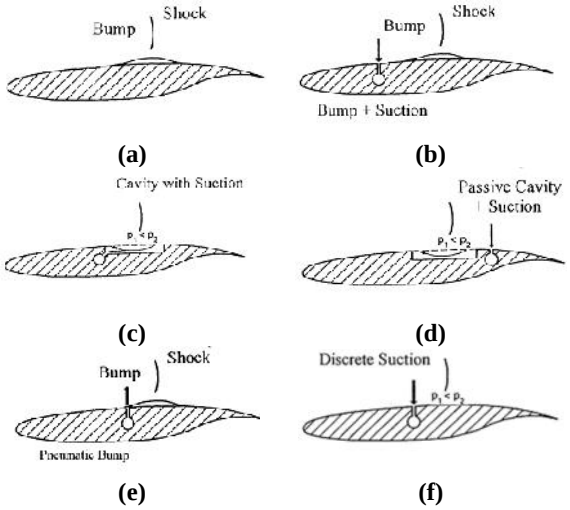

Fig. 1 Euroshock presented methods to reduce shock wave related drags

Two main active methods include surface mass transfer and local surface geometry improvement. The latter could be achieved by applying a set of actuators which could deform the flexible skin of the wing. The main principle of this method and pneumatic bump or surface flow injection is that by changing the slope of the local surface near the location of the shock wave, the isentropic compression waves will be created and thus there is a condition for Mach decrement of flow upstream the shock wave [1].

It was experienced that doing the suction upstream the shock wave does not have a positive effect on the wave drag decrement while it may also increase the shock wave strength instead. However, since this method has the potential to control boundary layer growth when encountering the shock wave, it can reduce the viscous drag and consequently decrease the total drag. The hybrid control method using the bump and upstream suction has the advantage of boundary layer thinning; hence after the bump position and shock wave occurrence, the separation will be reduced [1].

In the suction/injection control method, the main principle to control the shock wave boundary layer interaction is to increase the total energy in the boundary layer so that it can overcome the adverse pressure gradient across the shock wave. This can be achieved by mass injection or mass removal. Mass removal by the fluid suction on the airfoil surface as a method to control shock boundary layer interaction has been studied widely ([3], [4]). Although with suction, the boundary layer is thinner and the shock wave is more stable and normal, and thus its strength would be increased, it also results in wave drag increment. This can also be noticed in numerical studies of Qin et al's [5]. Mass injection for control of the shock wave was investigated by Wong [6] experimentally.

Qin et al.'s [7] studies indicate that suction generally promotes airfoil aerodynamic performance by increment in the lift to drag ratio. This is while it increases shock wave strength and leads it downstream. Fluid injection upstream the shock wave, reduces the shock wave strength noticeably by creation of the Lambda wave or compression waves. Other references concerning the subject of transonic flow control using surface mass transfer are in the area of their optimization. Yagiz and Kandil [8] optimized the suction and injection transonic flow control parameters using a gradient based method. As an another example of the latest researches in the area of the active flow control optimization, one can mention the study of Pehlivanglou and Yagiz [9] which by the use of a surrogate based Genetic Algorithm optimization method, optimization of airfoil shape, multi-elements airfoils and also active flow control in the transonic regime has been done.

The main purpose of this study is a due parametric study of suction/injection parameters such as its location, angle and strength to gain an insight into the level of importance of each parameter for NACA64A010 airfoil in a predetermined flow condition and also to determine the required information to commence an optimization process.

2 Governing Equations

The computational code applied to solve the problem of surface mass transfer is what is developed in [10]. The conservative form of two dimensional unsteady compressible Navier-Stokes equations is used to model the high Reynolds number turbulent flow as the following:

$$\frac{\partial Q}{\partial t}+\frac{\partial F}{\partial x}+\frac{\partial G}{\partial y}=0 \qquad (1)$$

Where Q is the array containing the conserved variables and F and G contain the Cartesian components of the flux vector which include convective and viscous flux:

$$F=F^I-F^V,\quad G=G^I-G^V \qquad (2)$$

Superscripts I and V are used to separate inviscid and viscous terms. The finite-volume method applied to the governing mean-flow equations in integral conservation form can be obtained by integrating the governing equations over the domain of interest Ω and applying the Gauss theorem to the second term of equation:

$$\frac{d}{dt}(Q_i A_i)+R_i(Q)-D_i(Q)=0 \qquad (3)$$

A_i is the area of the cell i. The artificial dissipation fluxes $D_i(Q)$ consists of a blending of a second order term to diminish oscillation around discontinuities such as shock wave and a forth order term to damp high oscillations in domain. It is added due to the central difference nature of our discretization. In order to get a fully implicit method the Eq. (3) could be rewritten as:

$$\frac{d}{dt}(A_i\ Q_i)+R_i(Q^{n+1})-D_i(Q^{n+1})=0 \qquad (4)$$

where superscript n+1 shows the time step $(n+1)\Delta t$ and d/dt has been modeled using an implicit second order backward difference so that:

$$\frac{3}{2\Delta t}(A_i^{n+1}Q_i^{n+1})-\frac{2}{\Delta t}(A_i^{n}Q_i^{n})+\frac{1}{2\Delta t}(A_i^{n-1}Q_i^{n-1})+R_i(Q^{n+1})-D_i(Q^{n+1})=0 \qquad (5)$$

Equation (5) for Q_i^{n+1} is a system of non-linear differential equations and cannot be solved with analytical methods. In this step by the definition of unsteady residual R^* as:

$$R_i^*(Q^{n+1})=R_i(Q^{n+1})-D_i(Q^{n+1})+A_i\left[\frac{3}{2\Delta t}(Q_i^{n+1})-\frac{2}{\Delta t}(Q_i^{n})+\frac{1}{2\Delta t}(Q_i^{n-1})\right]=0 \qquad (6)$$

and writing the differential equation with respect to imaginary time ² that the above equation is its steady state answer:

$$A_i\frac{\partial Q_i^{n+1}}{\partial ²}+R_i^*(Q^{n+1})=0 \qquad (7)$$

One can integrate the above equation in imaginary time ² and obtain its steady state answer which is Eq. (5) answer in real time step. In this study the system of Eq. (7) has been integrated using four-step explicit method in imaginary time. In addition, because the steady state answer is required, all the convergence acceleration methods such as residual smoothing and local time stepping could be applied. These methods reduce the computational time. Further details about the method can be found in [10].

Turbulence effects can be taken into account by using a suitable turbulence model. In this paper, two-equation k-epsilon turbulence model developed with Launder and Spalding [11] has been applied. The wall-function approach is adopted to treat the near-wall region of the boundary layer [10]. In this approach the quantities of interest are evaluated as functions of mean-flow quantities according to the law-of-the-wall. This approach is computationally very efficient, since a highly-refined computational grid is not required in the near-wall region.

2.3 Initial and boundary conditions

The initial conditions (t=0) applied in the present method consist of setting all the quantities equal to their free stream values. The wall boundary condition is the no-slip condition, which states that at the wall the velocity is zero.

On the part of airfoil with mass transfer, the velocity normal component is computed as:

$$u_N=\frac{C_Q\,°_\infty U_\infty c}{\sum_{L_{\text{mass transfer}}}°_w\Delta s} \qquad (8)$$

where suction/injection coefficient is defined as:

$$C_Q = \frac{\dot{m}}{\rho_\infty U_\infty c} = \frac{1}{\rho_\infty U_\infty c}\int_{s_1}^{s_2} \rho_w u_N ds \qquad (9)$$

In addition to the normal velocity component, the tangential component is determined by the suction/injection inclination angle which is in the range of 0 to 180 degrees to the airfoil surface. Positive C_Q coefficients indicate injection and negative amounts are indications of suction. Knowing the normal and tangential velocity component, their corresponding values in the Cartesian system are:

$$\begin{aligned} u &= -u_N \frac{\Delta y}{\Delta l} + u_T \frac{\Delta x}{\Delta l} \\ v &= u_N \frac{\Delta x}{\Delta l} + u_T \frac{\Delta y}{\Delta l} \end{aligned} \qquad (10)$$

Moreover, on the locations of airfoil with surface mass transfer, turbulent flow quantities are set by knowing the wall velocity so that $k_{wall} = 0.000025\left(u_{wall}^2 + v_{wall}^2\right)$ is the turbulent kinetic energy on the aforementioned locations. It should be mentioned that on the airfoils surface with mass transfer, the wall function treatment is switched off.

Since the main interest of the present method is the computation of high Reynolds number compressible turbulent flows, and since the viscous effects are present only in regions very far from the outer boundary, it is reasonable to apply the characteristic-based boundary conditions developed for inviscid flows.

3 Parametric Study Results

In this section, a thorough investigation of different suction and injection parameters and their level of efficiency on pressure coefficient distribution and thus airfoil aerodynamic performance have been carried out. The results are presented in two separate sections for suction and injection implementation and in each one the suction/injection coefficients and its inclination angle and location have been studied. The definitions for suction and injection inclination angles are given in Fig. 2.

Fig. 2 Definitions for suction and injection inclination angles

The results have been achieved for variation of only one parameter while two other parameters are considered to be fixed. The test case is carried out on NACA64A010 airfoil in 2.9 million Reynolds number, 0.5 degree angle of attack and 0.78 Mach number whom experimental data are available through Smith and Walker [4]. A 195×73 nodes grid with first cell distance of 0.0001 which represents the y^+ values of 10 on the airfoil surface is found to be suitable for this case after a systematic grid study (Fig. 3). A typical convergence behavior of the mean and turbulent flow variables are shown in Fig. 4.

The comparison of the lift and drag coefficients with other numerical results [7], in case of no suction, are presented in Table 1 with reasonable accuracy. In the presence of suction, the computed lift coefficient has higher accuracy than other numerical references. However, the computed drag coefficient shows greater error which may be due to the use of the wall function approach near the surface.

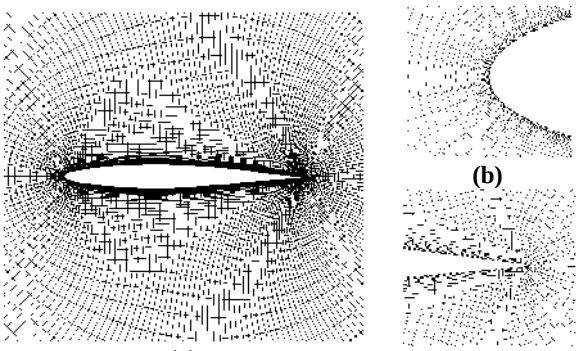

Fig. 3 a) NACA64A010 Hyperbolic grid b) leading-edge zoom b) trailing-edge zoom

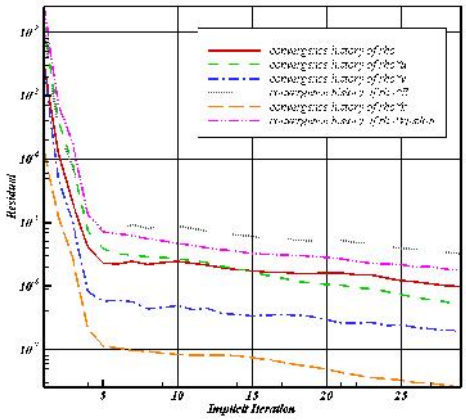

Fig. 4 Convergence history of mean and turbulence flow variables

Table 1 Investigation of lift and drag coefficients sensitivity to grid size

	Grid Size	C_L	C_D
Without suction	195×73	0.2012	0.0139
	Experiment [4]	0.2000	0.0130
	Numerical [7]	0.2166	0.0111
With suction	195×73	0.2645	0.0151
	Experiment [4]	0.2400	0.0140
	Numerical [7]	0.2795	0.0138

Airfoil surface pressure distributions with and without surface suction in comparison with the experimental results for 195×73 grid and by one and three cells on the suction location, is given in Fig. 5 showing good agreement with the corresponding experimental data.

The skin friction coefficient distribution with and without suction is compared in Fig. 6 showing a sudden increment in suction location due to increasing the velocity gradient by sucking in the low energy flow of the boundary layer. The velocity vectors at 69 to 72.5 percent of the chord are illustrated in Fig. 7 that show the velocity gradient increase on the airfoil boundary.

The Mach contours with and without surface suction are given in Fig. 8 showing a shock strength increase with suction and its movement downstream.

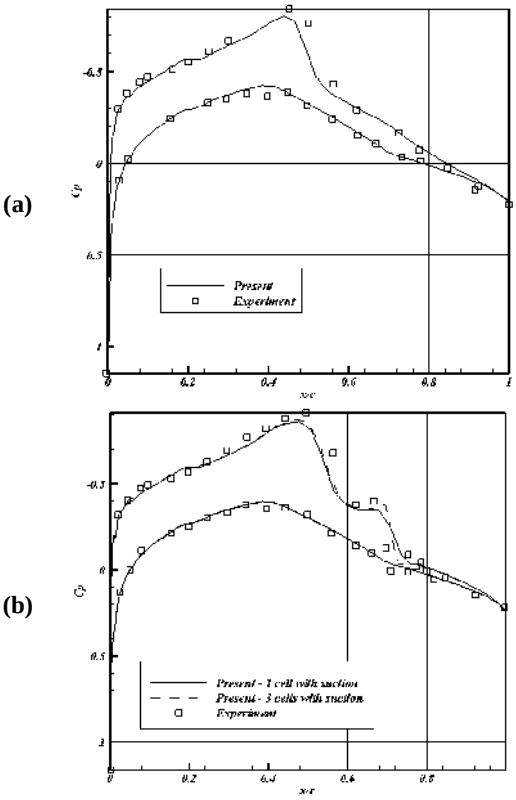

Fig. 5 NACA64A010 pressure distribution a) without suction b) with suction

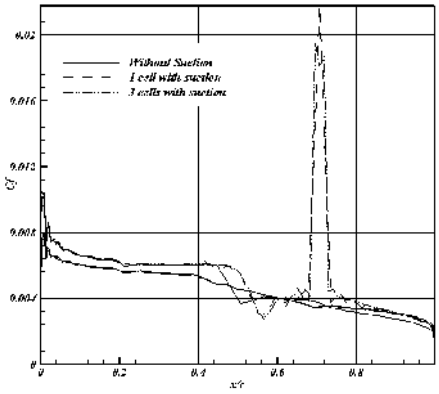

Fig. 6 . NACA64A010 skin friction coefficient with and without suction

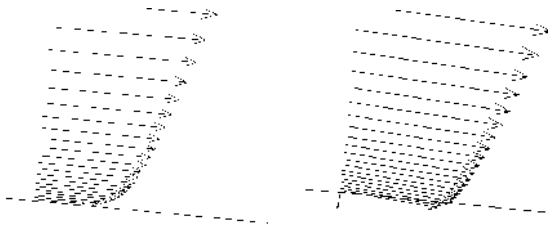

(a) **(b)**

Fig. 7 NACA64A010 velocity vectors a) without suction b) with suction at 69 to 72.5 percent of the chord

(a)

(b)

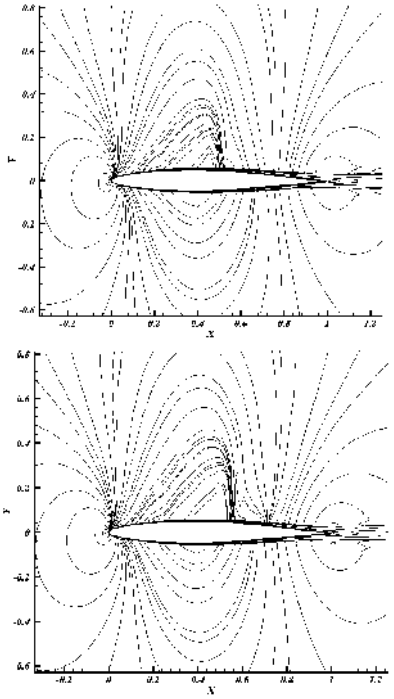

Fig. 8 NACA64A010 Mach contours a) without suction b) with suction

3.1. Suction Parametric Study

The suction coefficient variations in the range of 0.001- 0.004 are studied in the airfoil mid location of $x/c = 0.504$ to $x/c = 0.531$ with a 90 degree inclination angle. As it can be seen in Fig. 7, this location is directly on the shock wave foot and a bit downstream of it. In Fig. 9, the pressure coefficient and lift and drag coefficients and their ratio variations with the change in suction coefficient are presented. As it was mentioned earlier, the use of suction generally increases airfoil lift that is due to removal of separated flow caused by the shock wave. On the other hand, the suction employment causes velocity gradient augmentation on the surface that leads to the increase of skin friction drag and by the increase in wave drag due to shock wave strength, results in a total drag increase.

The results show that increasing the suction coefficient, increases the lift and drag coefficients accordingly. However, their variations are so that the aerodynamics efficiency factor (Cl/C_d) has an initial increase and then decreases steadily (Fig. 9 part (d)). The surface pressure coefficient distributions (Fig. 9) show that by increasing the suction coefficient, the shock wave becomes more stable and normal so that the drag coefficient dominated by the wave drag will increase linearly. However, the lift coefficient variation is somehow different. As it can be noticed from pressure coefficient distribution plots, further strong suctions no longer cause lift increment and thus result in the aerodynamic efficiency factor decrease.

(a)

(b)

(c)

(d)

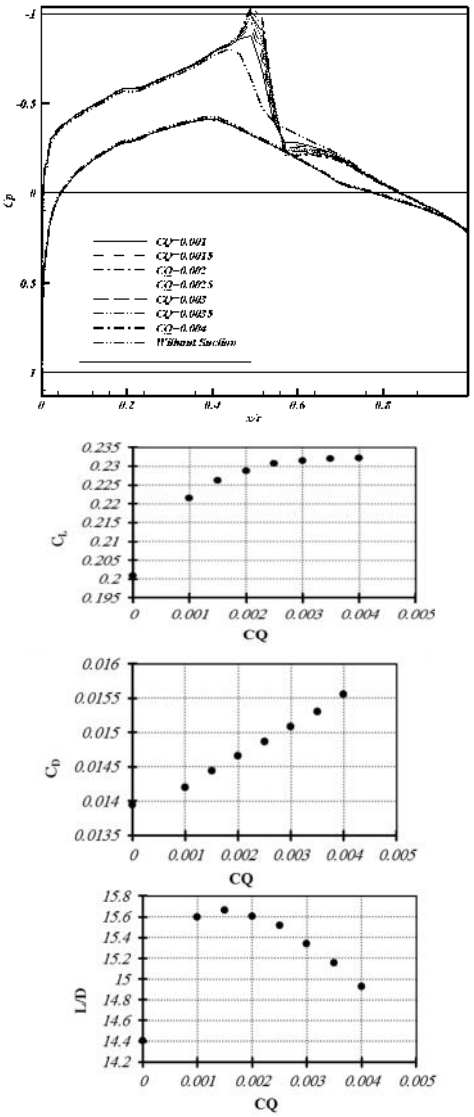

Fig. 9 Suction coefficient study

Suction inclination angle investigation has been carried out downstream the shock wave occurrence on the airfoil where the suction location is considered in $x/c = 0.771$ to $x/c = 0.797$ and with a suction coefficient of

0.002. The range of variation of the inclination angle is considered from 2 to 178 degrees. In Fig. 10, the surface pressure coefficient distributions and the corresponding lift and drag coefficients are plotted against the suction angle.

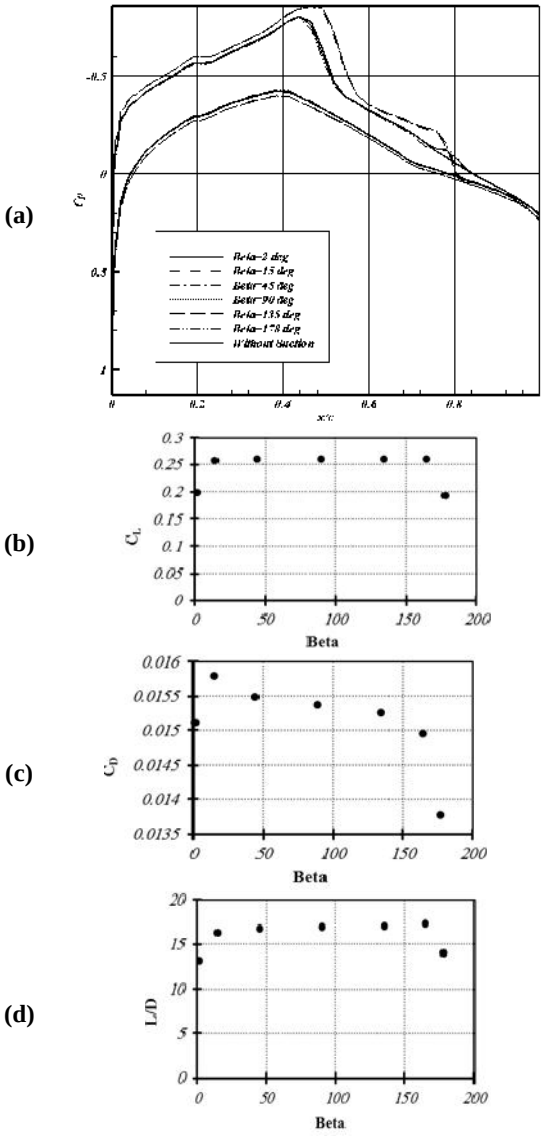

Fig. 10 Suction angle study

It can be noticed that low suction angles do not have any remarkable effect on the airfoil lift coefficient. From the other point of view, with inclination angle changes between 45 to 135 degrees, the airfoil lift and drag and their ratio are independent of suction angle. It should be noted that low suction angles (i.e 2 degree) are representative of tangent suction opposite the flow direction and angles close to 180 degrees are representative of tangent suction in the flow direction so that they cause a lower velocity gradient and lower skin friction drag.

The suction location has been studied with a constant suction coefficient of 0.002 and a 90 degree inclination angle. Five locations are selected for this study. In Fig. 11 the surface pressure coefficients and the corresponding lift and drag coefficients and their ratio are shown with the suction locations. In this figure, the location numbers 1 and 2 are related to the upstream of the shock wave, 3 on the shock wave foot and 4 and 5 downstream the shock wave. It should be noted that location 0 corresponds to the no suction case.

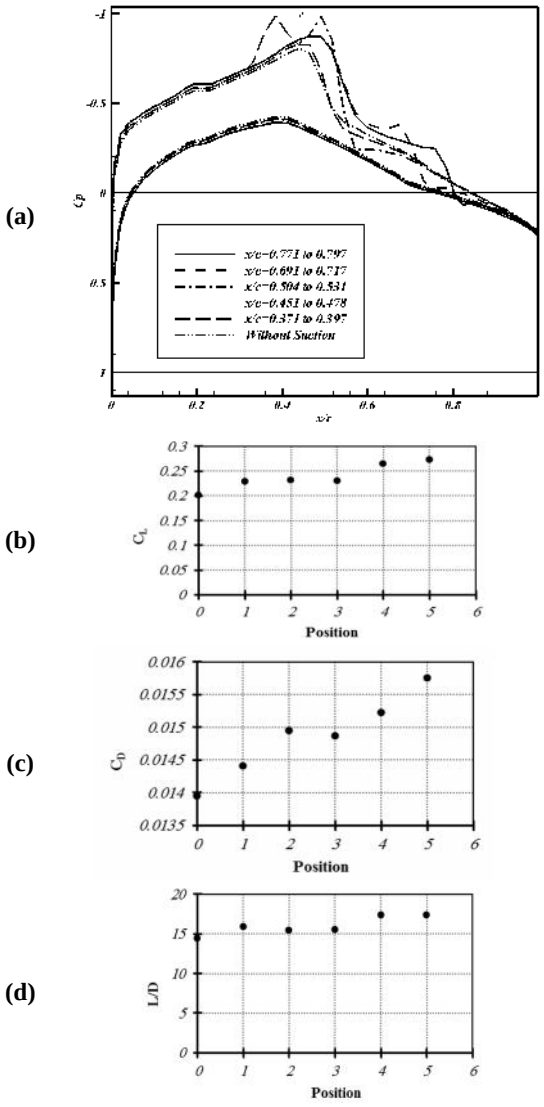

Fig. 11 Suction location study

The results show that as the suction location moves towards the shock wave position, the shock wave moves more downstream and its strength increased so that the wave drag is increased. The lift coefficient exhibits only a minor change with suction location changes up to the shock wave position. The drag coefficient however, shows a greater increase which is mainly due to increasing the shock wave strength.

Application of suction downstream the shock wave where its interaction with boundary layer occurs has a major effect. For instance, the lift coefficient will increase noticeably due to the shock wave moving downstream. All in all, suction implementation downstream the shock wave position, improves airfoil aerodynamic performance by about 15%.

3.2. Injection Parametric Study

The injection parametric study again consists of investigation about the effects of three different parameters; the injection coefficient, injection angle and injection location while in each study only one parameter is left to be variable and the other two parameters are fixed.

The injection coefficient study is carried out in the same manner as suction coefficient study, i.e. the injection is made in the airfoil mid-section $x/c=0.504$ to $x/c=0.531$ with a 90 degree inclination angle. The considered range of injection coefficient is 0.0002-0.001. It is noted that the injection coefficient is normally lower than suction coefficient level because the surface injection acts as a pneumatic bump on airfoil and its strength has a great impact on the airfoil behavior [7]. In Fig. 12, lift, drag, surface pressure coefficients and lift to drag ratio are shown in contrast to the injection coefficient. As a result of the injection, a bit downstream of the shock wave location on the surface, the shock will move upstream that causes an airfoil pressure drag increase. Again due to upstream movement of the shock wave and upper surface pressure increase, the airfoil lift coefficient will decrease. Therefore, from Fig. 12 part (d) it can be concluded that the surface injection downstream the shock wave has no favorable effect on the aerodynamic efficiency of the airfoil.

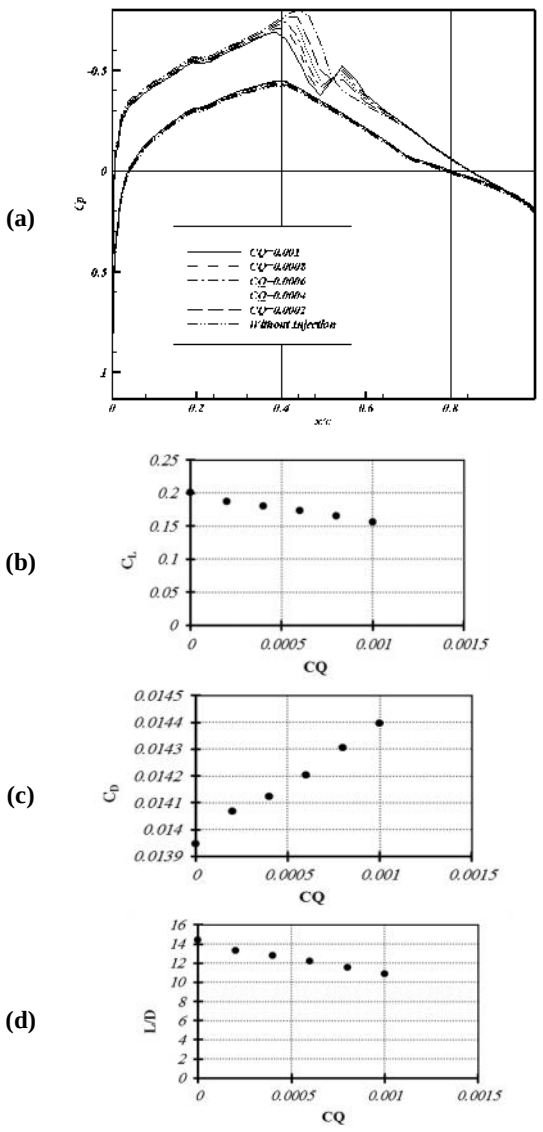

Fig. 12 . Injection coefficient study

The injection inclination angle study has been carried out again in the airfoil mid-section where injection has been applied in $x/c=0.504$ to $x/c=0.531$ with a 0.0006 injection coefficient and the considered range for inclination angle was 2-178 degrees.

Fig. 13 shows the main aerodynamic characteristics of the flow against the injection angle. It can be seen that the injection angle similar to suction angle, does not have a great impact on the airfoil aerodynamic performance except the jet injecting tangent to the surface

into the boundary layer that has opposite effects on the drag coefficient.

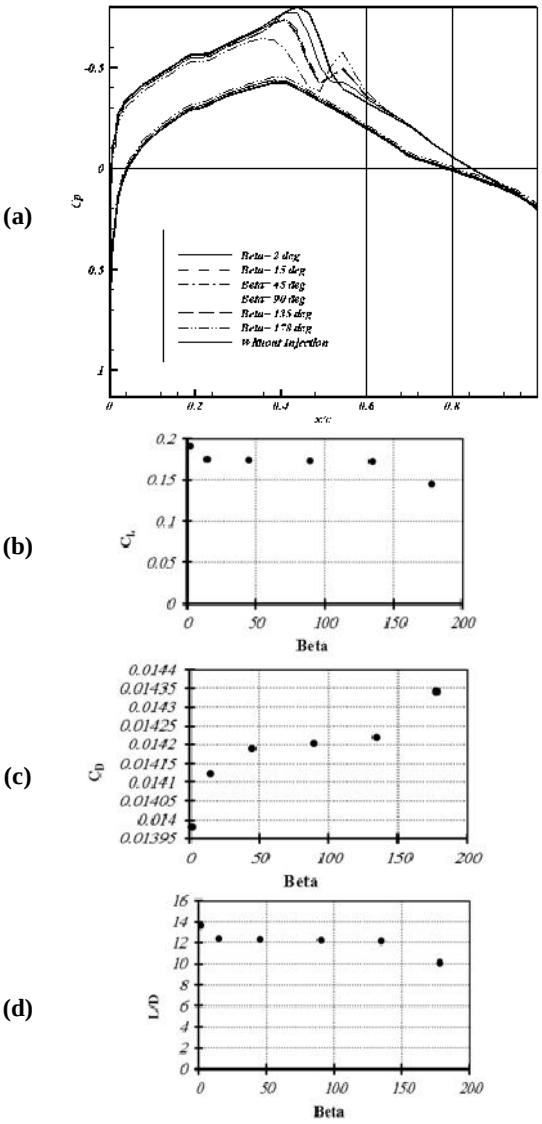

Fig. 13 . Injection angle study

Injection location is investigated by its application with a 0.006 coefficient and 90 degree inclination angle at 5 locations similar as it was applied for suction and the corresponding results are shown in Fig. 14. The effects of injection location, similar to suction location, depend on shock wave occurrence position. Injection implementation in location number 1 where it is fairly far upstream the shock wave location has no effect on the shock wave and just makes a pressure change locally. But in location numbers 2 and 3 which are closer and upstream the shock wave, the shock wave has weakened and the wave drag is reduced. Location numbers 4 and 5 which are downstream the shock wave, have an equal effect on shock wave strength and just cause changes in pressure locally as it can be seen from the pressure distribution. All in all, the lift and drag coefficients are decreased so that the L/D amounts are remained unchanged.

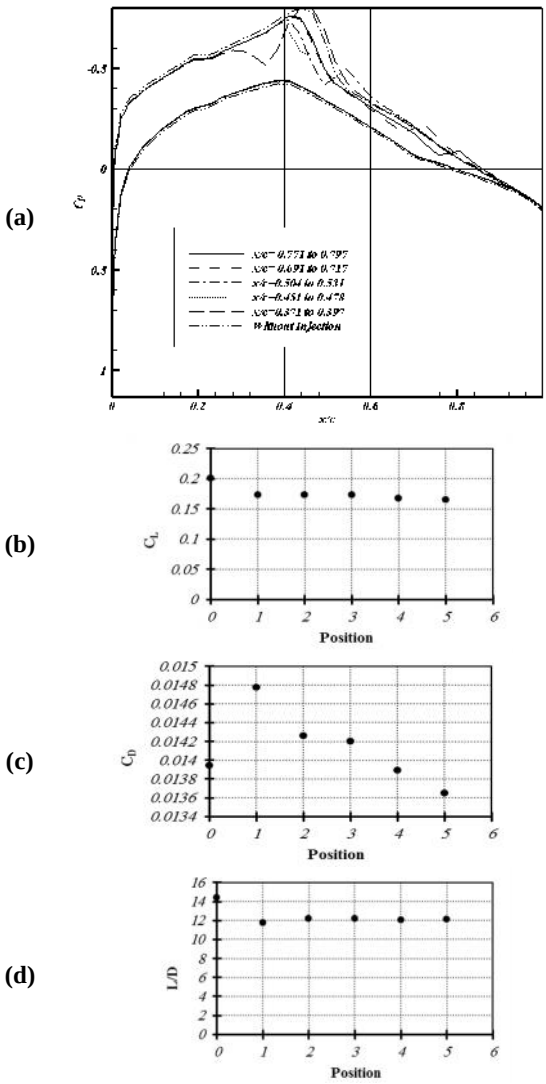

Fig. 14 Injection location study

An illustration of Mach contour before injection implementation and after that at location 5 is illustrated in Fig. 15 that shows reduction in shock strength and its movement to upstream.

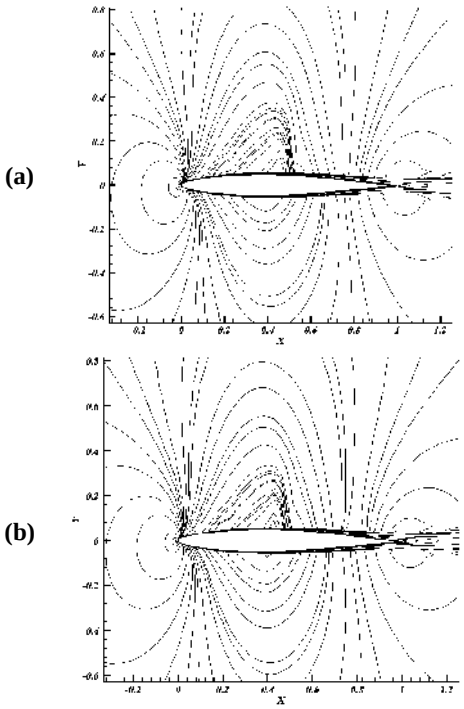

Fig. 15 NACA64A010 Mach contours a) without injection b) with injection

4 Conclusions

In this paper, a dual-time implicit finite volume method has been employed to solve the compressible turbulent flows around airfoils with surface mass transfer. A parametric study was then carried out in order to further understand the impacts of the suction/injection parameters on the transonic flow control especially at off-design conditions. It was concluded that the suction/injection location relative to the shock wave location has a major impact on the transonic flow control mechanism and also on the lift and drag coefficients. The results also show the different abilities of the active flow control by surface mass transfer.

References

[1] Stanewsky E, Delery J, Fulker J and de Matteis P. *Drag reduction by shock and boundary layer control, (Results of project Euroshock II supported by the European Union 1996-1999)*. Springer, Heidelberg, 2002**.**

[2] Delery JM. Shock wave/turbulent boundary layer interaction and its control. *Progress in Aerospace Sciences*, Vol. 22, pp 209-280, 1985.

[3] Delery JM. Shock phenomena in high speed aerodynamics: still a source of major concern. *The Aeronautical Journal*, Vol. 103, No.1019, pp 19-34, 1999.

[4] Smith DW and Walker JH. *Test of an area suction flap on a NACA64A010 airfoil at high subsonic speeds*, *NASA TN D 310*, 1960.

[5] Qin N, Zhu Y and Poll DIA. Surface suction on aerofoil aerodynamic characteristics at transonic speeds. *Proceedings of the Institution of Mechanical Engineers, Part G: Journal of Aerospace Engineering*, Vol. 212, pp 339-351, 1998.

[6] Wong W.F. Application of boundary layer blowing to suppress strong shock induced separation in a supersonic inlet. *AIAA 15th Aerospace Sciences Meeting*, pp 77-147, 1977.

[7] Qin N, Zhu Y and Shaw ST. Numerical study of active shock control for transonic aerodynamics. *International Journal of Numerical Methods for Heat & Fluid Flow*, Vol. 14, No. 4, pp 444-466, 2002.

[8] Yagiz B and Kandil O. Optimization of active flow control in transonic aerodynamics. *27th AIAA Applied Aerodynamics Conference*, 2009.

[9] Pehlivanoglu V and Yagiz B. Aerodynamic design prediction using surrogate-based modeling in genetic algorithm architecture. *Aerospace Science and Technology*. Vol. 23, pp 479-491, 2012.

[10] Jahangirian A and Hadidoolabi M. Unstructured moving grids for implicit calculation of unsteady compressible viscous flows. *International Journal for Numerical Methods in Fluids*, Vol. 47, No. 10/11, pp 1107–1113, 2005.

[11] Launder BE and Spalding DB. The Numerical Computation of Turbulent Flows, *Computer Methods in Applied Mechanics and Engineering*, Vol. 3, pp 269-289, 1974.

Contact Author Email Address

mailto: ajahan@aut.ac.ir

Copyright Statement